http://ansinet.com/itj

ITJ

ISSN 1812-5638

INFORMATION TECHNOLOGY JOURNAL

ANSInet
Asian Network for Scientific Information
308 Lasani Town, Sargodha Road, Faisalabad - Pakistan

Information Technology Journal 12 (24): 8235-8241, 2013
ISSN 1812-5638 / DOI: 10.3923/itj.2013.8235.8241

Numerical Analysis of Stress in the Large Permanent Magnet Motor Stator Cores Including Magnetostriction Effects

Xin Zhang, Qingxin Yang and Xian Zhang
Key Laboratory of Advanced Electrical Engineering and Energy Technology,
Tianjin Polytechnic Universitym, 300387, Tianjin, China

Abstract: Noise suppression is one of the important issues to be solved in the motor design and application. Dominant electromagnetic noise in the low-speed case, magnetostrictive force account for a large proportion for the generation of electromagnetic noise and vibration and this phenomenon is particularly prominent in large motors. In this study, the impact of the rotating magnetic field to magnetostrictive properties of the permanent magnet motor stator core is analyzed. Through the quadratic moment domain rotation model, a rotating magnetic field of the magnetic-mechanical coupled numerical model is built. Under the permanent magnet motor stator boundary conditions, the electromagnetic field distribution is constructed, stator cores magnetostrictive stress, strain and displacement are calculated by FEM and the distribution of stress is obtained on the permanent magnet motor stator teeth. This study provides an effective numerical method for the design of large-scale high-performance permanent magnet motor with low noise.

Key words: PMSM, magnetostriction, electromagnetic noise, quadratic moment domain rotation model

INTRODUCTION

Magnetic forces and magnetostriction in electrical machines are the main reason for the generation of electromagnetic vibration and noise (Belahcen, 2004). Magnetic forces are the reluctance forces acting at the interface between two mediums of different permeabilities. Magnetostriction is magnetostrictive forces acting on ferromagnetic region due to the change in the permeability. The change in the permeability of the medium is caused by stress on the material, the phenomenon commonly known as inverse magnetostriction effect. The origin of research on the motor electromagnetic noise is in the 1940s.

Recent studies have basically focused on the magnetic forces that magnetostrictive contribution to electromagnetic noise is considered small. The books of Gieras *et al.* (2005) comprehensively discusses the calculation of the electromagnetic force, the impact of the inverter, torque ripple, noise and vibration analysis, numerical analysis, statistical energy analysis, noise control as well as mechanical and aerodynamic noise.

Until the early 2000s some new points on this issue appear. Professor Osama A. Mohammed' teams (Mohammed *et al.*, 2001, 2003, 2005) at Florida International University research the stator silicon steel deformation caused by magnetostriction. The 2D nonlinear static and transient finite element model is established, on which the motor stator stress is analyzed, magnetic force and the deformation of stator caused by magnetostriction is computed and the impact of rotating magnetic field on magnetostriction is discussed. The result indicate that magmetostrictive forces are significant and amount to more than 50% force level increase above electromechanical force levels obtained without accounting for magnetostriction.

In recent years, the research on electromagnetic noise and vibration of motor had been reported, based on steady-state and transient model considering the magnetostrictive effect (Hilgert *et al.*, 2007; Le Besnerais *et al.*, 2010; Leleut *et al.*, 2005). Belahcen (2004) builds a mathematical model considering transient magnetostrictive effect and separately calculates the magneto-mechanical coupling and magnetostriction (Wang *et al.*, 2009; Chang-Liang *et al.*, 2001). These methods generally consists of several steps: first, measure magnetic and magnetostrictive properties of the silicon steel; second, build electromagnetic field-mechanical coupled numerical model; third, analyze motor modal and solve the displacement of vibration. A finite-element investigation has shown that the contributions to vibration of a large electrical machine from Maxwell forces in the air gap and the magnetostriction effect in the stator cores are comparable (Shahaj and Garvey, 2011).

Corresponding Author: Xin Zhang, Key Laboratory of Advanced Electrical Engineering and Energy Technology, Tianjin Polytechnic University, 300387, Tianjin, China

Magnetostriction can act either to reduce or increase the overall modal excitation compared to the excitation of Maxwell forces.

This study proposes a 2D numerical model of permanent magnet motor, using quadratic moment domain rotation model approximate magneto-strictive linear elastic properties of the material. Anisotropic properties of silicon steel in rotating field are obtained by means of vector transform. Under the permanent magnet motor stator boundary conditions, the electromagnetic field distribution is constructed, stator cores magnetostrictive stress, strain and displacement are calculated by FEM and the distribution of stress is obtained on the permanent magnet motor stator teeth. To a certain extent, this study promotes the progress of low-noise motor design and high-performance motor drive applications.

MATHEMATICAL MODELS

Stator cores silicon steel magnetic- mechanical coupled numerical model: Linear magnetostrictive material constitutive relation equation can be expressed as (Clark, 1980):

$$\varepsilon_H = \sigma/E_{\sigma=}+dH \quad (1)$$

$$B_\sigma = \mu_\sigma H+d\sigma \quad (2)$$

where ε_H is the material total strain when the magnetic field strength is H, E_σ is Young's modulus, σ is the stress tensor, d is the magnetostrictive coefficient, H is the magnetic field, B_σ is the Magnetic flux density under stress, μ_σ is the permeability under stress.

Based on quadratic moment domain rotation model, Magnetostriction of the isotropic material and magnetization have the following approximately relationship under certain stress (Chikazumi, 1997):

$$\lambda = \frac{3}{2}\lambda_s\left[\left(\frac{M}{M_s}\right)^2 - \frac{1}{3}\right] \quad (3)$$

where, λ is the Magnetostriction; λ_s is the saturation magnetostriction; M is the Magnetization; M_s is the saturation magnetostriction.

When considering the nonlinear magnetic hysteresis, in Eq. 1, the second term of the right side of the formula can be expressed as the magnetostriction with magnetic hysteresis and Eq. 4 can be obtained:

$$\varepsilon_H = \sigma/E_\sigma+\lambda \quad (4)$$

Magnetic flux density can be expressed as:

$$B = \mu_0 (M+H) \quad (5)$$

Substituting (3) into Eq. 4 and 5 compose of the magnetic hysteresis nonlinear pressure equation, Eq. 6 can be expressed as:

$$\begin{aligned}&\varepsilon_H = \sigma / E_\sigma + \frac{3}{2}\lambda_s\left[\left(\frac{M}{M_s}\right)^2 - \frac{1}{3}\right]\\ &B = \mu_0 (M + H)\end{aligned} \quad (6)$$

It can be seen that B and μ are changed due to the mechanical deformation and the stress on the material conversely change the permeability. Electromagnetic and mechanical coupling is achived.

Anisotropy of the material in the field of rotating machinery: In the stationary magnetic field, silicon steel stator reluctance can be measured, the four components v''_{xx}, v''_{xy}, v''_{yx}, v''_{yy}. As described in the study (Enokizono *et al*., 1997), reluctance ν in rotating magnetic field can be solved through vector conversion. φ is the angle of the ellipse of the rotary magnetic flux density and the direction of the spindle, the axial ratio of the ellipse $\rho = B_{min}/B_{max}$ and the rotating magnetic reluctance is obtained:

$$\begin{bmatrix} \nu_{xx} & \nu_{xy} \\ \nu_{yx} & \nu_{yy} \end{bmatrix} = T\begin{bmatrix} 1 & 0 \\ 0 & \rho \end{bmatrix}\begin{bmatrix} \nu'_{xx} & \nu''_{xy} \\ \nu''_{yx} & \nu'_{yy} \end{bmatrix}\begin{bmatrix} 1 & 0 \\ 0 & \rho \end{bmatrix}^{-1} T^{-1} \quad (7)$$

Where:

$$\begin{bmatrix} \nu'_{xx} & \nu'_{xy} \\ \nu'_{yx} & \nu'_{yy} \end{bmatrix}$$

is the round stationary magnetic flux density reluctance matrix:

$$T = \begin{bmatrix} \cos\phi & -\sin\phi \\ \sin\phi & \cos\phi \end{bmatrix}$$

is the coordinate conversion factor.

Taking into account the material anisotropy of the mechanical rotation field and $H = \nu B$, solving Maxwell's equations in the region of the stator cores, the Eq. 8 can be obtained:

$$\begin{aligned}&\frac{\partial}{\partial x}(\nu_{yy}\frac{\partial A}{\partial x}) + \frac{\partial}{\partial y}(\nu_{xx}\frac{\partial A}{\partial y}) - \frac{\partial}{\partial x}(\nu_{yx}\frac{\partial A}{\partial y})\\ &-\frac{\partial}{\partial y}(\nu_{xy}\frac{\partial A}{\partial x}) = J_e\end{aligned} \quad (8)$$

where, A is Magnetic vector potential, ν_{xx}, ν_{xy}, ν_{yx}, ν_{yy} are the reluctance component, J_e is excitation current density.

As a result of the finite element discertization, the following matrix equations for both the electro- magnetic and mechanical problems can be obtained:

$$[S]\,[A] = [J_e] \tag{9}$$

$$[K]\,[U] = [F] \tag{10}$$

When using the finite element calculations, separately solving the electromagnetic and mechanical stiffness matrix, the stationary point of the energy functional is written as (Mohammed, 2001):

$$I_{Mag}(A) = \int_R (\int_0^B H^T \cdot dB)dR - \int_R J_e \cdot A dR \tag{11}$$

$$\begin{aligned} I_{Mec}(U) = &-\int_V \frac{1}{2}\varepsilon(U)^T \cdot \sigma(U)dV \\ &-\int_V f_V \cdot U dV - \int_\Gamma f_\Gamma \cdot U d\Gamma \end{aligned} \tag{12}$$

where f_v is the external volume force density, f_Γ is the external surface force density, U is the displacement, R is the magnetic region, V is the mechanical domain volume, Γ is the boundary of mechanical volume and T stands for vector transpose. The relationship between stress and strain is $\sigma = D\varepsilon$, Where D is the stiffness matrix for the 2D elastic material that can be expressed as:

$$D = \frac{E}{(1+\alpha)(1-2\alpha)}\begin{bmatrix} 1-\alpha & \alpha & 0 \\ \alpha & 1-\alpha & 0 \\ 0 & 0 & (1-2\alpha)/2 \end{bmatrix} \tag{13}$$

where, α is Poisson's ratio.

Based on the energy minimization principle, discreting the magnetic energy functional, Eq. 14 can be expressed as:

$$\begin{aligned} \frac{\partial I_{Mag}(A)}{\partial A_i} = &\int_R v_{yy}\frac{\partial A}{\partial x}\cdot\frac{\partial}{\partial A_i}\frac{\partial}{\partial x}dR \\ &+\int_R v_{xx}\frac{\partial A}{\partial y}\cdot\frac{\partial}{\partial A_i}\frac{\partial}{\partial y}dR \\ &-\int_R v_{xy}\frac{\partial A}{\partial y}\cdot\frac{\partial}{\partial A_i}\frac{\partial}{\partial x}dR \\ &-\int_R v_{yx}\frac{\partial A}{\partial x}\cdot\frac{\partial}{\partial A_i}\frac{\partial}{\partial y}dR \\ &-\int_R J_e\frac{\partial A}{\partial A_i}dR = 0 \end{aligned} \tag{14}$$

Discreting the mechanical stress field energy functional, Eq. 16 can be expressed as:

$$\begin{aligned} \frac{\partial I_{Mec}(U)}{\partial U_i} = &\int_V \frac{1}{2}\sigma(U)\cdot\varepsilon(U)dV \\ &-\int_V f_V\frac{\partial U}{\partial U_i}dV \\ &-\int_\Gamma f_\Gamma\frac{\partial U}{\partial U_i}d\Gamma = 0 \end{aligned} \tag{15}$$

where, $A = [A_1, A_2 \ldots A_m]$, , $U = [U_1, U_2 \ldots U_n]$.

m and n are separately number of total node in the region for calculating the magnetic field and stress field. Sequential solve two Eq. 9 and 10 and achieve iteration through Eq. 6.

SIMULATION RESULTS AND ANALYSIS

This study chooses a four-pole surface mounted permanent magnet synchronous motor model as an object, performs transient numerical calculations, shown in Fig. 1. The rotor rotates clockwise and counterclockwise in turn. The sampling time is set to [0-0.25] for a period of revolution of the motor.

Boundary conditions: In Fig. 1, the blue circle is the fixed constraints of the stator periphery.

Initial conditions: In Fig. 1, the orange area is a region of the ferromagnetic rotor, in which the initial stress and the strain are zero. The green area and the blue area are separately the permanent magnet N and S poles. The gray area is the inner stator ferromagnetic region, in which the initial stress is zero and the initial strain is λ_i, as in Eq. 16 shown below:

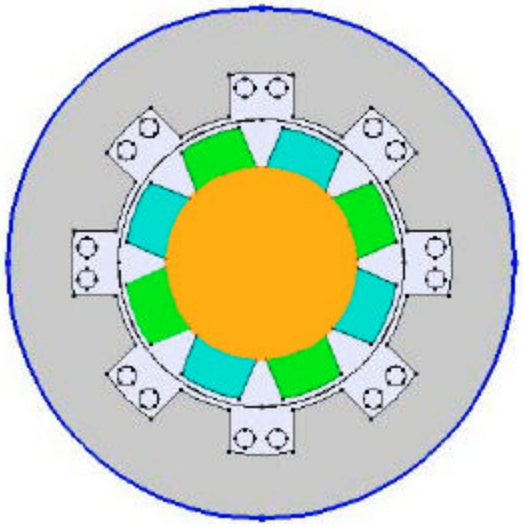

Fig. 1: Fixed constraints of the stator periphery

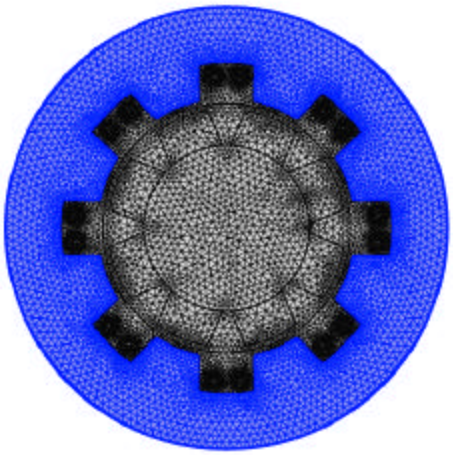

Fig. 2: Schematic diagram of the stator cores mesh

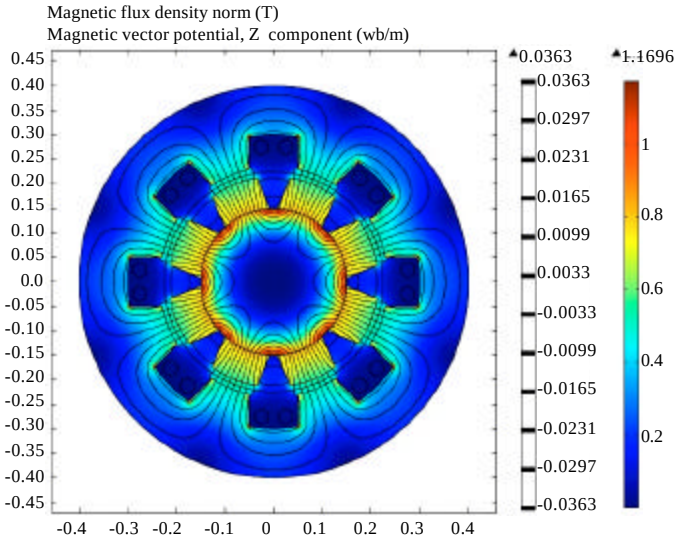

Fig. 3: Magnetic flux density and the magnetic potential without magnetostrictive effect at time 0

$$\lambda_i = \frac{3}{2}\lambda_s\left[\left(\frac{M_i}{M_s}\right)^2 - \frac{1}{3}\right];\quad i = x, y \tag{16}$$

Split results: The blue part of Fig. 2 is mesh of stator cores.

Magnetic field simulation results: Figure 3 and 4 show simulation results of the magnetic flux density and the magnetic potential without magnetostrictive effect. In Fig. 5 and 6, the results consider the magnetostrictive effect. All calculation use the M-19 electrical steel curve data (Enokizono *et al*., 1997).

In Figures magnetic flux density changes color from blue to red and magnetic potential is the black flow lines. As can be seen, at different times, the distributions of the magnetic flux density are different on surfaces of the teeth or in the inner area of the stator cores, wherein the base and the top of the stator teeth flux density are larger. For consideration of the magnetostrictive effect of Fig. 5 and 6, the stator teeth have obvious deformation.

Stress simulation results of the special points: Extracted from the result of the calculation of stress in a relatively large number of special stress points shown in Fig. 7, select 32 (blue), 38 (green), 42 (cyan), 41 (red), 32 and 42 located stator tooth roots, 38 and 41 located at the top of the stator teeth.

The diagram of specific point stress in stator teeth can be obtained, shown in Fig. 8 and 9. The stator frequency of the stress variation is twice the rotational

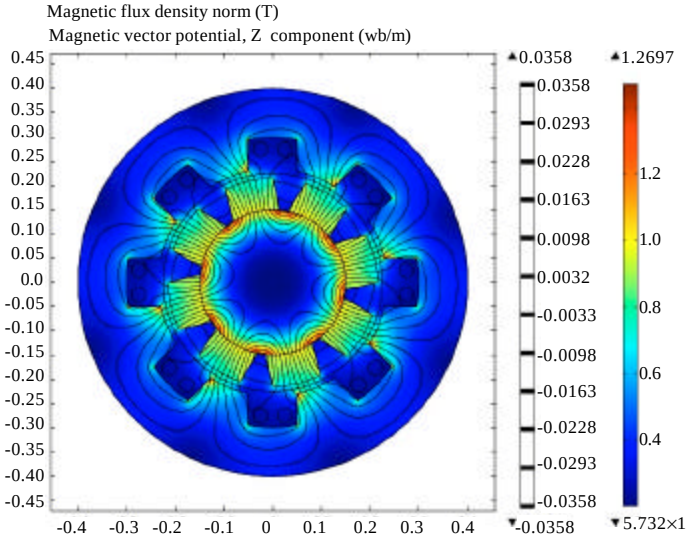

Fig. 4: Magnetic flux density and the magnetic potential without magnetostrictive effect at time 0.1

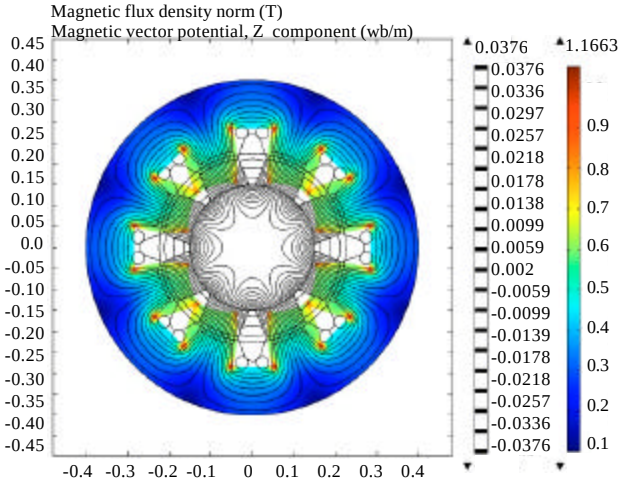

Fig. 5: Magnetic flux density and the magnetic potential considering magnetostrictive effect at time 0

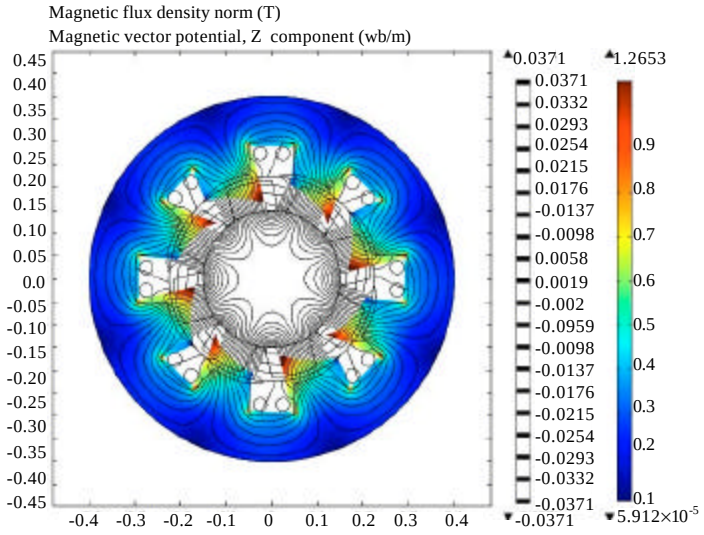

Fig. 6: Magnetic flux density and the magnetic potential considering magnetostrictive effect at time 0.1

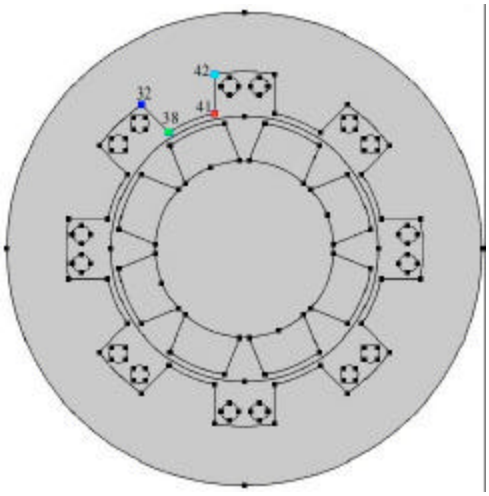

Fig. 7: Stress analysis point selection

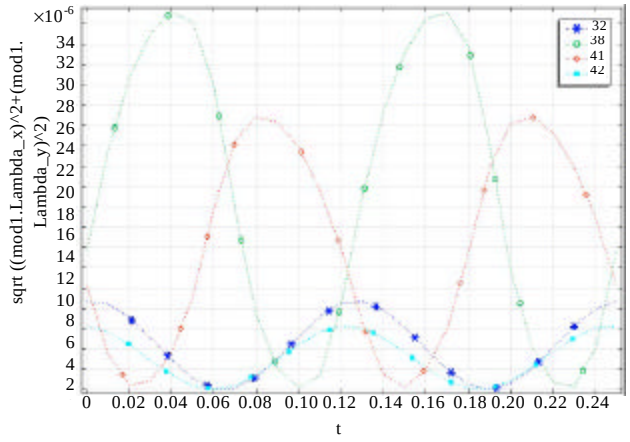

Fig. 8: Stator tooth special point stress change map when motor rotate counterclockwise

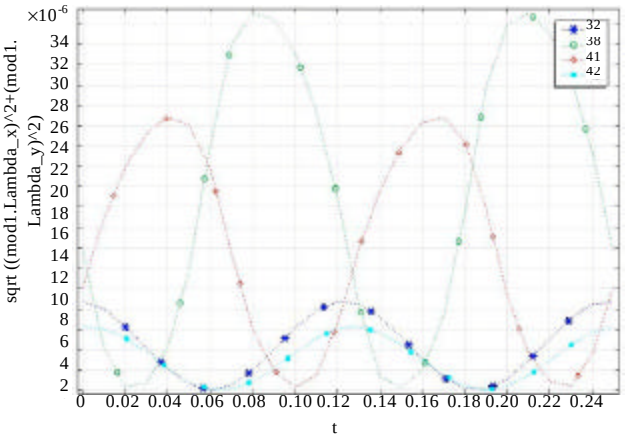

Fig. 9 Stator tooth special point stress change map when motor rotate clockwise

speed of the motor. The stress modulus values of stator teeth root is less than the one of the stator teeth top. With different magnetic motor rotation direction, the stator teeth stress modulus value is unchanged and the phase is different. Taking into account the reluctance of stator cores silicon steel (ν''_{xx}, ν''_{xy} ν''_{yx} ν''_{yy}) associated with silicon steel sheet rolling direction, resulting stress modulus values are different in the stator teeth top special point 41 and 38 the same as root special point 32 and 42 .

CONCLUSION AND SUMMARY

Based on electromagnetic theory, the theory of elasticity and coordinate transformation, this study analyze impact of the rotating magnetic field of the permanent magnet motor stator cores silicon steel magnetostrictive properties, use quadratic moment domain rotation model, build the magnetic-mechanical coupled numerical mode under the rotating magnetic field, obtain the electromagnetic field distribution of permanent magnet motor stator under boundary conditions, magnetostrictive stress, strain and displacement of the permanent magnet motor stator tooth by means of finite element calculation. The results show that due to the magnetostrictive effect of the stator cores in the rotating magnetic field will produce deformation, stress in stator tooth top is lager than the one in root and stress modulus value has nothing to do with the motor rotation direction. The method is important of analyzing large permanent magnet motor design phase stress magnitude and distribution. This study provides a theoretical basis for the analysis methods and programs to reduce electromagnetic noise.

ACKNOWLEDGMENTS

The Project was supported by the State Key Program of National Natural Science of China (Grant No. 51237005). The Project was supported by the National Natural Science Foundation of China (Grant No. 51307120).

The Project was supported by the State Key Program of Foundation of Tianjin (Grant No. 12JCZDJC28600).

The Project was supported by Science and Technology Planning Project of Tianjin, China (Grant No. 20130416).

REFERENCES

Belahcen, A., 2004. Magnetoelasticity, magnetic forces and magnetostriction in electrical machines. Ph.D. Thesis, Helsinki University of Technology, Finland.

Chang-Liang, X., Z. Yao and S. Ting-Na, 2001. FEM analysis of stator vibration of traveling wave type contact ultrasonic motor. Proc. Chin. Soc. Electr. Eng., 21: 25-28.

Chikazumi, S., 1997. Physics of Ferromagnetism. Oxford University Press Inc., New York.

Clark, A.E., 1980. Magnetostrictive Rare Earth-Fe2 Compounds. In: Ferromagnetic Material, Wohlforth, E.R. (Ed.). North-Holland, Amsterdam.

Enokizono, M., S. Mori and O. Benda, 1997. A treatment of the magnetic reluctivity tensor for rotating magnetic field. IEEE Trans. Magn., 33: 1608-1611.

Gieras, J.F., C. Wang and J.C. Lai, 2005. Noise of Polyphase Electric Motors. CRC Press, New York, ISBN: 9781420027730, Pages 392.

Hilgert, T.G., L. Vandevelde and J.A. Melkebeek, 2007. Numerical analysis of the contribution of magnetic forces and magnetostriction to the vibrations in induction machines. Sci. Meas. Technol. IET, 1: 21-24.

Le Besnerais, J., V. Lanfranchi, M., Hecquet and P. Brochet, 2010. Characterization and reduction of audible magnetic noise due to PWM supply in induction machines. IEEE Trans. Ind. Electron., 57: 1288-1295.

Leleut, E., C. Espanet, A. Miraoui and S. Siala, 2005. Reduction of vibrations in an induction machine supplied by high power PWM inverter. Proceedings of the European Conference on Power Electronics and Applications, September 2005, Dresden, Germany, pp: 1-8.

Mohammed, O.A., T.E. Calvert, L. Peterson and R. McConnell, 2003. Transient modeling of magnetoelastic problems in electric machinery. Applied Comput. Electromagnet. Soc. J., 18: 77-83.

Mohammed, O.A., 2001. Coupled magnetoelastic finite element formulation of anisotropic magnetostatic problems. Proceedings of the IEEE SoutheastCon , 30 March-01 April , 2001, Clemson, South Carolina, pp: 183-187.

Mohammed, O.A., N.Y. Abed, S. Liu and S. Ganu, 2005. Acoustic noise signal generation due to magnetostrictive effects in electrical equipment. Proceedings of the 22nd National Radio Science Conference, March 15-17, 2005, Cairo, Egypt, pp: 45-52.

Mohammed, O.A., T. Calvert and R. McConnell, 2001. Coupled magnetoelastic finite element formulation including anisotropic reluctivity tensor and magnetostriction effects for machinery applications. IEEE Trans. Magn., 37: 3388-3392.

Shahaj, A. and S.D. Garvey, 2011. A possible method for magnetostrictive reduction of vibration in large electrical machines. IEEE Trans. Magn., 47: 374-385.

Wang, W., Z.H. Song, J. Chen, S.B. Yu and R.Y. Tang, 2009. The calculation of natural frequencies of stator system and electromagnetic acoustic noise of AFIR disc PM machine. Electr. Mach. Control 13: 857-861.